



**HAL**  
open science

# On the collision quenching of by N<sub>2</sub> and O<sub>2</sub> and its influence on the measurement of E/N by intensity ratio of nitrogen spectral bands

G Dilecce, P F Ambrico, S de Benedictis

► **To cite this version:**

G Dilecce, P F Ambrico, S de Benedictis. On the collision quenching of by N<sub>2</sub> and O<sub>2</sub> and its influence on the measurement of E/N by intensity ratio of nitrogen spectral bands. *Journal of Physics D: Applied Physics*, 2010, 43 (19), pp.195201. 10.1088/0022-3727/43/19/195201 . hal-00569602

**HAL Id: hal-00569602**

**<https://hal.science/hal-00569602>**

Submitted on 25 Feb 2011

**HAL** is a multi-disciplinary open access archive for the deposit and dissemination of scientific research documents, whether they are published or not. The documents may come from teaching and research institutions in France or abroad, or from public or private research centers.

L'archive ouverte pluridisciplinaire **HAL**, est destinée au dépôt et à la diffusion de documents scientifiques de niveau recherche, publiés ou non, émanant des établissements d'enseignement et de recherche français ou étrangers, des laboratoires publics ou privés.

# On the collision quenching of $\text{N}_2^+(B^2\Sigma_u^+, v = 0)$ by $\text{N}_2$ and $\text{O}_2$ and its influence on the measurement of E/N by intensity ratio of nitrogen spectral bands

G Dilecce<sup>1,2,‡</sup>, P F Ambrico<sup>1</sup> and S De Benedictis<sup>1</sup>

<sup>1</sup>Istituto di Metodologie Inorganiche e dei Plasmi-CNR, sede di Bari, Via Orabona, 4, 70126 Bari - ITALY

<sup>2</sup>Istituto di Fotonica e Nanotecnologie-CNR, sede di Trento, Via alla Cascata 56/C, 38050 Povo - Trento - ITALY

**Abstract.** Laser induced fluorescence measurements of the rate coefficients of  $\text{N}_2^+(B^2\Sigma_u^+, v = 0)$  collision quenching by  $\text{N}_2$  and  $\text{O}_2$  are presented. The values of  $(8.84 \pm 0.37) \times 10^{-10} \text{cm}^3 \text{s}^{-1}$  and  $(10.45 \pm 0.45) \times 10^{-10} \text{cm}^3 \text{s}^{-1}$  have been found for  $\text{N}_2$  and  $\text{O}_2$  respectively. The present results agree well with literature data obtained by selective methods for ion B state excitation. The data are discussed in the frame of the spectroscopic evaluation of the reduced electric field in electrical discharges at high pressure, that makes use of the Second Positive System (SPS) and First Negative System (FNS) emissions of nitrogen.

PACS numbers: 39.30.+w, 52.70.kz, 52.80.-s

*Keywords:* Spectroscopic Techniques, Plasma Diagnostics, LIF,

‡ corresponding author: giorgio.dilecce@ba.imip.cnr.it

## 1. Introduction

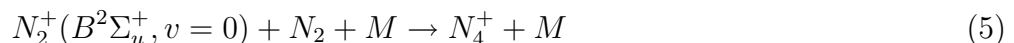
The determination of the electric field strength in a discharge by spectroscopic methods is an old issue [1] that is nowadays receiving renewed attention, in both low and high pressure discharges [2], [3]. In air or, more generally, in nitrogen containing discharges, this is achieved by looking at emissions belonging to the Second Positive System (SPS) of  $N_2$ :  $C^3\Pi_u \rightarrow B^3\Pi_g$  and to the First Negative System (FNS) of  $N_2^+$ :  $B^2\Sigma_u^+ \rightarrow X^2\Sigma_g^+$ . The intensity ratio of these two emissions is very sensitive to the mean electron energy, and then to the reduced electric field  $E/N$ , due to the large difference of excitation thresholds of the two excited states, 11.03 eV for  $N_2(C^3\Pi_u, v = 0)$  and 18.7 eV for  $N_2^+(B^2\Sigma_u^+, v = 0)$  (bands belonging to  $v=0$  vibrational quantum number of both electronic states are usually employed). The emission ratio is proportional to the ratio of the populations of the emitting states. Populations are calculated at the stationary state as the ratio of excitation and quenching rates. Excitation rates are calculated by solving the Boltzmann equation with the proper cross sections, with the reduced electric field -  $E/N$  - as a parameter, in the hypothesis of local field approximation - LFA (for example with a Boltzmann solver like BOLSIG+ [4]). Another working hypothesis is that both  $N_2(C^3\Pi_u)$  and  $N_2^+(B^2\Sigma_u^+)$  are excited by electron impact with ground state nitrogen molecules:



$E/N$  is deduced from the best match of calculated and measured SPS and FNS emission ratio. This method has been recently reviewed and analysed thoroughly in [5], in a wide pressure range, from 300 to  $10^5$  Pa. The relevant cross sections and collision quenching data typically adopted can be found there. As pressure increases the collision quenching,



overcomes the radiative quenching and becomes dominant at atmospheric pressure for both emitting states. The accurate knowledge of collision quenching rate constants is then of fundamental importance. In [5] the data of [6] and [7] were adopted for the collision quenching of  $N_2(C^3\Pi_u)$  and  $N_2^+(B^2\Sigma_u^+)$  respectively. Later in [8] it was pointed out that the associative ion conversion



with its  $5 \times 10^{-29} cm^6 s^{-1}$  rate constants, becomes dominant at high pressure, and has to be taken into account in the calculation of the total quenching of the FNS emitter. In order to choose the collision quenching rate constants values, one has to deal with quite a large amount of literature. A good convergence of data is found about the

quenching of  $N_2(C^3\Pi_u, v = 0, 1)$  by  $N_2$  (see [9]), and by  $O_2$  (see [6]), and the data of [6] are a good choice. A refinement in the calculation of C state population can be achieved by taking into account also vibrational relaxation, that has been measured in [9], as it was done in [10]. Large discrepancies exist, instead, between the many measurements of rate constants for  $N_2^+(B^2\Sigma_u^+, v = 0)$  by  $N_2$  and  $O_2$ . We have reported in table I these literature data: rate constant values differ by about a factor four for nitrogen quencher and by about a factor two for oxygen quencher. In the table the data are listed according to the method used for the excitation of the electronic state of the nitrogen ion, and a further grouping is made according to the method being selective or non-selective. It is clearly seen that selective excitation methods, i.e. those based on the absorption of resonant radiation, give the largest values. Among the non-selective methods, i.e. those that excite the whole manifold of electronic states, pulsed discharge based methods give the lowest values, while continuous electron/proton beam and soft X-ray methods give intermediate values. It is quite evident that the rate constants values are dependent on the measurement method, and that the choice of the right value is a matter that deserves a thorough discussion. For instance at 1 atm of nitrogen, using the value of [7] leads to a total collision quenching, processes (3) plus (5), of about  $3.5 \times 10^{10} s^{-1}$ , that, with the data of [11] instead amounts to  $5 \times 10^{10} s^{-1}$ . The model calculation of the SPS and FNS emission ratio can then be affected by a factor 1.43 variation according to the choice of quenching rate constants. In the pulsed discharge method of [7] (and [6]) a fast rise and fall time voltage pulse, with duration of few tens of ns, was applied to produce a discharge with the fast ionization wave (FIW) mechanism. After discharge-off, the decay of the emission intensity was measured and fitted by a single exponential function to get the quenching rate. A weak point of this method is that in the FIW, as pointed out by the same authors in [6], the relaxation of the EEDF in the energy range for inelastic processes proceeds for a time comparable to that of depopulation of the investigated levels. In other words the excitation of electronic states is not totally switched off during the emission decay time, and this might lead to a possible slowing down of the depopulation itself, i.e. to an underestimation of the measured quenching rate constants. This was argued to be a minor effect in [6] on the basis of two identical quenching results obtained at two different discharge durations, i.e. at two different electron density and mean energy conditions. A strong point of the FIW excitation method was that, due to the short duration and low repetition rate of the discharge, the dissociation degree and the concentration of excited species is very low, so that it is possible to consider for the quenching the species and concentrations that constitute the initial gas feed only. Electron/proton beam based methods use a continuous beam for excitation of electronic species in a background gas. The emission intensity is then recorded as a function of the background gas. It is an indirect method since, in addition to the precise characterization of the electron beam characteristics, it requires to take into account the effect of excitation by low-energy secondary electrons coming from the ionizations produced by the principal beam. Such an effect depends on the background gas pressure. Finally resonant excitation methods

**Table 1.**  $N_2^+(B^2\Sigma_u^+, v = 0)$  quenching rate constants ( $10^{-10}cm^3s^{-1}$ ) by  $N_2$  and  $O_2$ . Present results and literature data. Data are grouped according to selective and non-selective excitation methods.

quencher		<i>ref.</i>	excitation method	sel./non sel.
$N_2$	$O_2$			
$8.84 \pm 0.37$	$10.45 \pm 0.45$	this work	resonant laser (LIF)	sel.
$8.2 \pm 1.2$		[11]	resonant laser (LIF)	
7.5	11	[12]	resonant radiation	
$5.4 \pm 1.0$		[13]	resonant radiation	
$3.9 \pm 1.4$		[14]	electron beam	non sel.
$4.3 \pm 0.27$	$7.2 \pm 3$	[15]	electron beam	
$(6.0 - 7.7) \pm 1.5$		[16]	electron beam	
3.66 (at 300 K)		[17]	electron beam	
4.15		[18]	pulsed proton beam	
4.53	7.36	[19]	soft X-ray	
$(1.37 - 2.17)$		[20]	pulsed discharge (invertron)	
$2.1 \pm 0.2$	$5.1 \pm 0.5$	[7]	pulsed discharge (FIW)	

are the most direct and less affected by spurious effects, since they are based on the measurement of the quenching rate of an excess population of the single vibronic state that is selectively excited by absorption of resonant radiation. In [11], laser radiation was used to excite  $N_2^+(B^2\Sigma_u^+, v = 0)$  from the ion ground state and the fluorescence pulse decay provided the quenching rate. A sufficient population of ions was produced in a continuous d.c. discharge. This is a possible weak point, since the exact gas composition in presence of gases that can be easily dissociated might not be neatly known. A possible role of quenching by electron impact was instead reasonably ruled out in [11]. In this paper we have revisited this subject by combining the cleanliness of laser induced fluorescence measurements with the advantage of production of ground state ions by means of a short duration, low repetition rate discharge, that are the same advantages as those described for the FIW excitation method. New data on  $N_2^+(B^2\Sigma_u^+, v = 0)$  quenching by  $N_2$  and  $O_2$  are provided that can help in the decision on which values to adopt in the application of spectroscopic methods to the E/N determination.

## 2. Experimental

### 2.1. discharge

The ground state nitrogen ions necessary for LIF process (see next section) are produced in a short pulse dielectric barrier discharge. A drawing of the electrodes arrangement is shown in figure 1. The bottom electrode is made of an alumina slab, 0.7 mm thick, with a  $8 \times 10$  mm rectangular surface covered by a silver loaded paint, on the side not exposed to the discharge. The top electrode is a bare, flat stainless steel disc in a ceramic holder. Both electrodes are mounted on sliding supports that allow to change the interelectrode distance under vacuum by computer controlled stepping motors. The whole apparatus

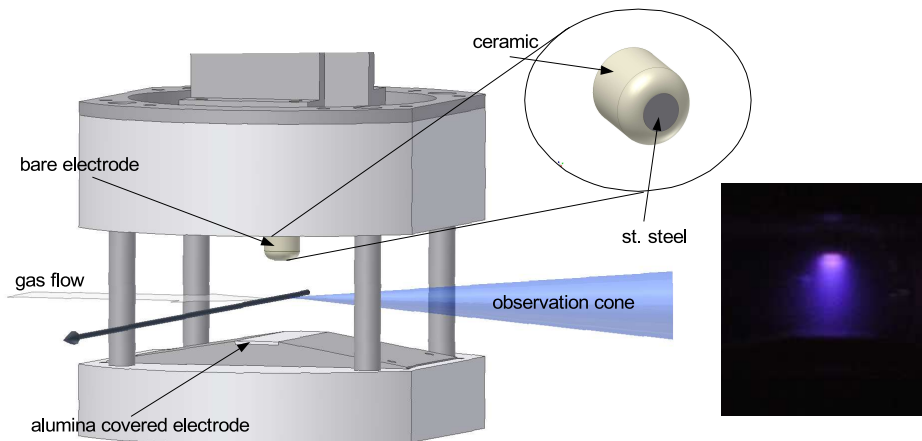


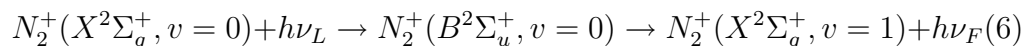
**Figure 1.** Sketch of the discharge hardware, with indication of the gas flow and LIF geometry (see text). In the annexed picture the discharge at 1.6 Torr is shown.

is described in more detail in [21].

The high voltage supply is composed of a low voltage pulse generator (TTi mod. TG1010A), a power amplifier (Industrial Test Equipment Powertron 1000A), and a HV transformer with an operating range 1-7 KHz, 25 kV max. voltage. A negative square pulse,  $10\mu s$  duration and 60 Hz repetition rate, is applied to the amplifier, resulting in a distorted waveform after the transformer, as shown in figure 2. In the same figure, as a monitor of the current, the discharge emission of the FNS (0,1) band is shown. The emission pulse is composed of a low initial part, lasting about  $5\mu s$ , followed by a more intense part that lasts about  $15\mu s$ . The LIF pulse is superimposed to the discharge emission, and its position marks the  $t=0$  point. The gas flow is operated by MKS flow meters/controllers, and pumping is achieved by a  $30\text{ m}^3/\text{h}$  rotary pump, that serves both for evacuating the vessel and for maintaining the dynamic pressure under gas flow by pumping through an adjustable needle valve.  $N_2$  and  $O_2$  (99.995% purity) are used, at a fixed flow rate of 50 sccm, in the pressure range 0.2-4 Torr. The pressure is measured by a capacitance manometer. We have used two gas compositions only: pure  $N_2$  and  $N_2 + 50\% O_2$ . In these conditions the interelectrode gap is fixed at 18 mm, while the peak negative voltage varies in the range 2-4 kV.

## 2.2. laser induced fluorescence

We have made mainly measurements of LIF pulses with large bandwidth detection, in order to measure the decay rate of the LIF pulse that carries the information on the collision quenching of the ion electronic state. Few fluorescence and emission spectra have also been recorded to explore the details of the LIF process under observation and to measure the gas temperature. The LIF excitation-detection scheme is as follows:



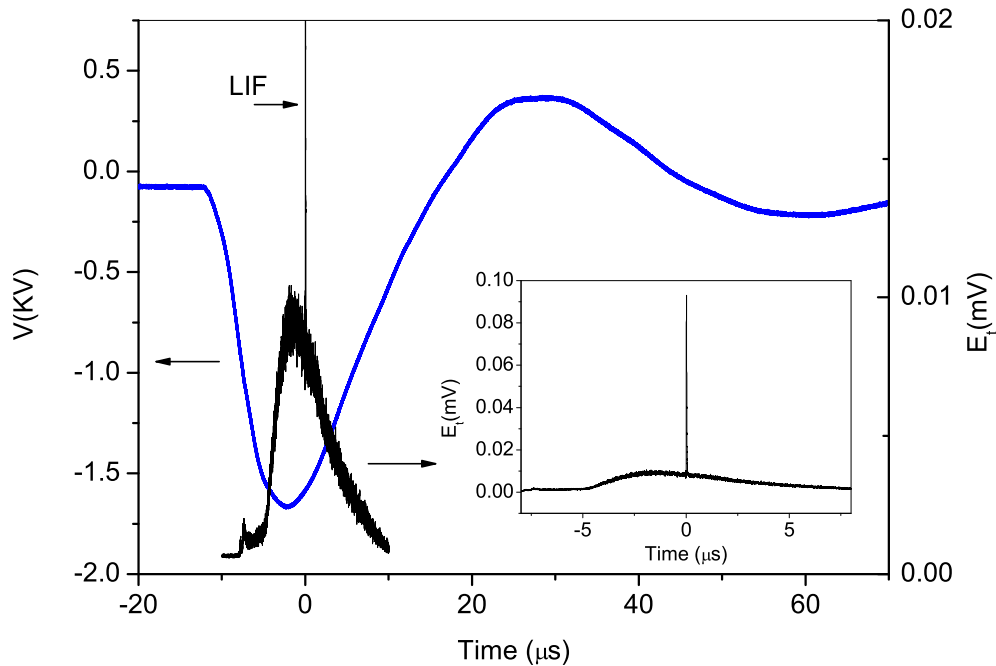


**Figure 2.** Oscillograms of the applied voltage and FNS (0,1) band emission in  $N_2$  at 2 Torr. The emission scale is compressed in the main figure. In the inset figure the whole emission plus LIF signals are shown in an uncompressed scale.

where  $\nu_L$  and  $\nu_F$  are the frequencies of the laser and fluorescence photons respectively. The laser apparatus consists of a Nd-YAG pumped tunable pulsed dye laser, with LDS 751 dye in DMSO solution, and a BBO second harmonic generator. The pulse width and energy are about 10 ns and 1 mJ respectively, at a wavelength of 391.424 nm, and the nominal bandwidth is  $0.4 \text{ cm}^{-1}$ , i.e. about 0.006 nm. The laser wavelength is measured with  $5 \times 10^{-6}$  relative accuracy by a High Finesse WS5 wavemeter. The excitation wavelength is chosen such as to maximize the fluorescence signal. It corresponds to a position close to the P-branch bandhead, with simultaneous excitation of  $N=10-16$  rotational levels. A fluorescence spectrum, measured at  $P=2$  Torr, is shown in figure 3. The spectrum is well reproduced by a simulation, calculated by LIFBASE [22], with the rotational distribution shown in the inset figure. Most of the fluorescence comes from the rotational levels  $N=10-16$  that are directly excited by the laser, while a weak collisional relaxation towards lower  $N$  levels is also present.

Both laser induced fluorescence and discharge emission light are collected perpendicularly to the laser beam, by a 1:1 telescope made of two 2 inches diameter, 30 cm focal length quartz lenses. Fluorescence spectra are measured by a 500 mm focal length SPEX 500M monochromator, equipped with two gratings, 600 gr./mm, 500 nm blaze and 1800 gr./mm 300 nm blaze, and an Andor DH5H7-18F-01 gated ICCD detector. Fluorescence pulses are instead measured by a Hamamatsu R2949 photomultiplier after spectral selection through a 1000 mm focal length McPherson monochromator with a 1200 gr./mm, 300 nm blaze grating with a choice of 0.2 mm and

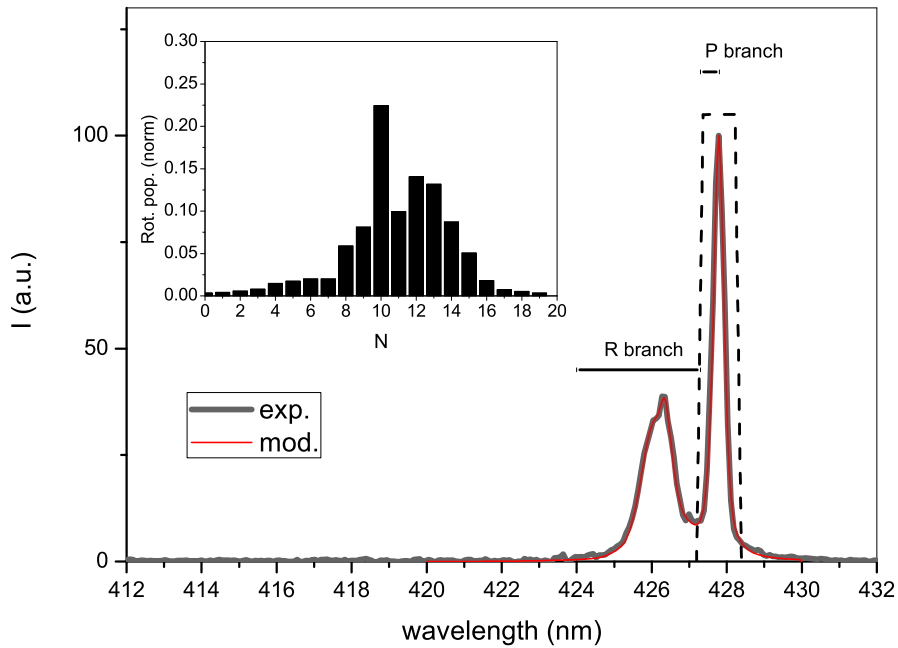


**Figure 3.** Fluorescence spectrum of FNS (0,1) band after laser excitation at 391.424 nm. The measurement is taken with the ICCD and a bandwidth of about 0.4 nm. The simulation is calculated by LIFBASE and with the rotational populations shown in the inset figure. The dashed lines define the position of the trapezoidal slit spectral transmission function used for LIF pulse measurements.

1 mm input and output slit width respectively. The trapezoidal spectral transmission function of the slits is positioned in such a way as to collect the whole P-branch rotational levels wavelengths that contribute to the LIF signal (see figure 3). With this setting there is no possibility of a spurious contribution to fluorescence decay due to some excitation that escapes the observation window by rotational relaxation. The current signal from the photomultiplier is measured by a digitizing oscilloscope (Le Croy waveRunner 6030A). The measurement output is a voltage vs. time signal. The voltage is the drop of the photomultiplier current across the  $50\Omega$  input impedance of the oscilloscope, and is then proportional to the number of photon/sec impinging on the photocathode. We will denote this quantity by  $E_t$ . The  $50\Omega$  input impedance of the oscilloscope is necessary to match the cable impedance and avoid reflections that could influence the measurement of the decay of such a fast signal. The laser firing, the ICCD gate and the oscilloscope are triggered by the discharge TTL trigger pulse.

### 2.3. Experimental method

The time resolved fluorescence pulses are recorded and their decay is fitted to a single exponential yielding the decay rate. In figure 4 a typical fluorescence pulse, both in linear and logarithmic scale is shown. Repeated measurements at various pressures allow construction of Stern-Volmer plots from which the rate constant is deduced. The concentration is calculated from the pressure after the measurement of the gas

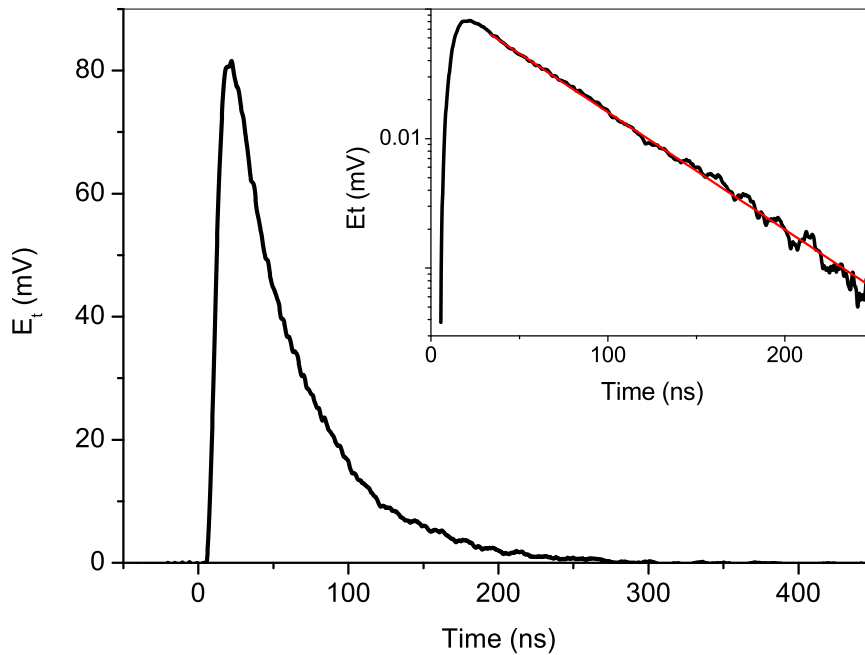


**Figure 4.** LIF pulse at  $P= 0.2$  Torr, pure  $N_2$  (after background subtraction). The curve shown is the average over 5000 laser shots. The same pulse is shown in logarithmic scale in the inset figure. Single exponential decay starts at about 30 ns, i.e. after about 20-25 ns from the beginning of the pulse. The red line is the exponential fit of the decay.

temperature. This is achieved by fitting the emission spectrum of FNS (0,0) band, as shown in figure 5.  $N_2^+(B)$  state is in fact excited from the ground state by electron impact, that is known to reproduce the ground state rotational distribution on the electronic excited state. The rotational distribution observed in FNS emissions is always Boltzmann-like, with a temperature of  $330 \pm 10$  K that is constant in all the pressure and gas composition conditions. We take this value as the gas temperature. In a few cases we have also verified that this value agrees well with that of  $N_2(C)$  state measured from SPS emission. LIF and gas temperature measurements are made at about  $8 \mu s$  after the discharge onset, as shown in figure 2. The short discharge duration and long time between two successive pulses prevents significant dissociation or formation of other species before the laser pulse. In [23] calculations and experiments in a pulsed d.c. discharge show that, in an air-like  $N_2$ - $O_2$  mixture, oxygen dissociation and NO formation are low at short pulse lengths. In particular, at pressures of the order of 0.1 Torr, O and NO fractional concentrations are less than  $10^{-3}$  for a pulse length of  $100 \mu s$ , the minimum length reported in that paper, with a fast rising trend with increasing pulse duration. It is then reasonable to assume that, in our case of  $8 \mu s$  discharge duration before the LIF measurement, dissociation and formation of other species is very low, and that, from the point of view of electronic states quenching, the concentration of quenchers is practically the same as that prepared by flow gas mixing and initially present at the discharge onset.

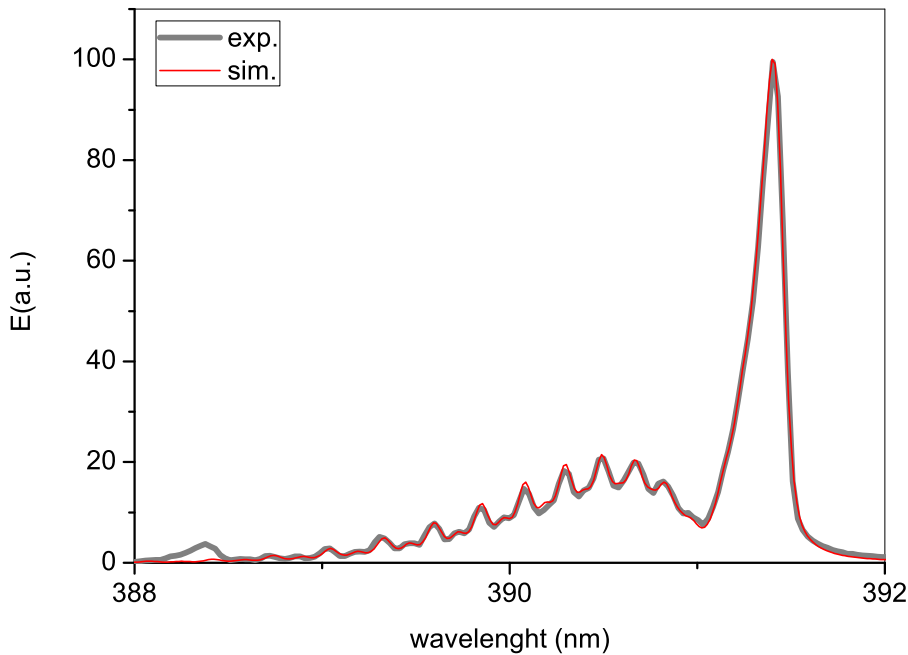


**Figure 5.** Emission spectrum of FNS (0,0) at 2 Torr of  $N_2+50\%O_2$ . The measurement is taken with the ICCD and the 1800 gr/mm grating, with a gate width of  $5 \mu s$  centered at the time of the laser shot. The simulation is calculated by LIFBASE with a Voigt instrumental profile (gaussian + 50 % Lorentzian), 0.12 nm bandwidth,  $T_{rot}=330K$

### 3. Results and discussion

The Stern-Volmer plots of the quenching rate as a function of pressure are reported in figure 6 and figure 7 for the pure  $N_2$  and for the  $N_2 + 50\% O_2$  mixture respectively.

The corresponding rate coefficients are reported in table 1, in which the error due to gas temperature uncertainty is included. The rate coefficient for quenching by  $O_2$  ( $k_{O_2}$ ) is calculated, after that by  $N_2$  ( $k_{N_2}$ ) has been determined, according to the simple relationship  $k_{mix} = \frac{1}{2}k_{N_2} + \frac{1}{2}k_{O_2}$ , where  $k_{mix}$  is the rate coefficient of the mixture determined from the slope of the plot of figure 7. The present results agree very well with all the literature data relevant to selective excitation methods, enforcing the idea that, as noted in the introduction, the measurement methods carry some systematic error that must be discussed in order to understand which values should be taken to be closer to real ones. From the point of view of E/N estimation from SPS and FNS emission measurements, this is not an irrelevant issue. We have estimated the effect of such indetermination in the case of a pure nitrogen discharge at atmospheric pressure. In this condition the total quenching rate of  $N_2^+(B^2\Sigma_u^+, v = 0)$  varies by about a factor 1.47 going from the lowest to the highest value of table 1 for the quenching rate coefficient. Given an experimentally determined  $[N_2^+(B)]/[N_2(C)]$  population ratio, the ratio of electron impact rate coefficients  $R = r_2/r_1$  deduced from the experimental population ratio using the quenching data of this work will be about 1.47 times larger than that

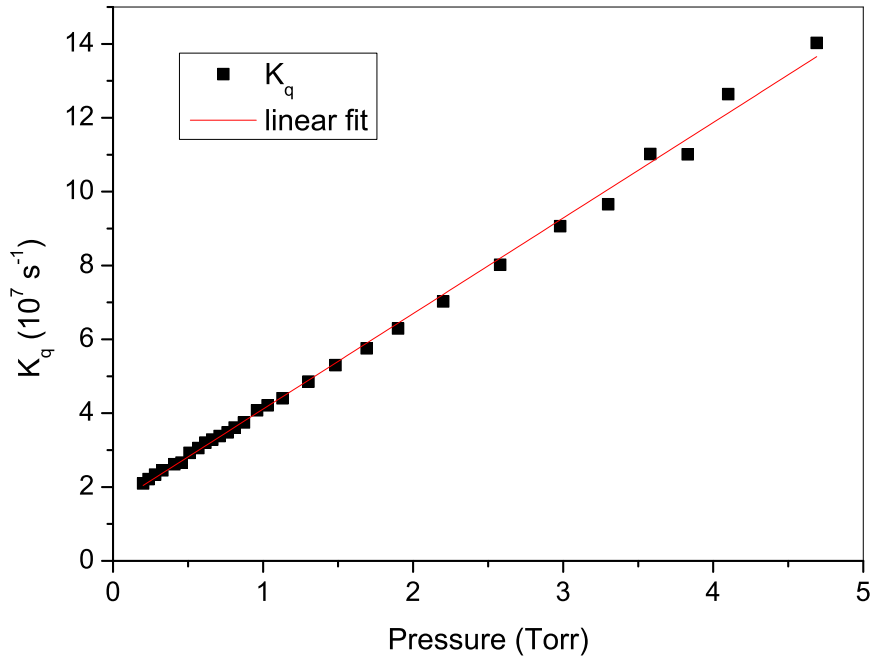


**Figure 6.** Stern-Volmer plot of the  $N_2^+(B^2\Sigma_u^+, v = 0)$  quenching rate in pure  $N_2$ . The linear fit gives a slope of  $(2.5871 \pm 0.027) \times 10^7 \text{ Torr}^{-1} \text{ s}^{-1}$  and an intercept of  $(1.5228 \pm 0.055) \times 10^7 \text{ s}^{-1}$ . The inverse of the intercept,  $\tau = 65.67 \pm 2.37 \text{ ns}$  is in good agreement with the 62.33 ns radiative lifetime of [24].

obtained by the data of [7], in nitrogen at one atmosphere. We have calculated by BOLSIG+ the ratio  $R$  as a function of  $E/N$  in pure nitrogen, and plotted  $E/N$  vs.  $R$  in figure 8. The error introduced by the factor 1.47 uncertainty in the quenching of the ion B state grows with growing  $E/N$ . In the figure three cases are shown graphically. Around  $E/N=100 \text{ Td}$  the indetermination in  $E/N$  amounts to about 8%, and grows to about 12% around  $E/N=200 \text{ Td}$  and to about 19% around 400 Td. The present measurements should be the most direct and less affected by collateral problems. The agreement with the data obtained by selective excitation is striking, for both  $N_2$  and  $O_2$  quenchers. As already stated in the introduction, a quick look at table 1 shows quite clearly that in each class of methods data are similar, and quite different from class to class. Each class of methods then could be affected by systematic errors ascribable to the method. Selective excitation gives the largest quenching values, therefore its possible systematic error would be an additional loss channel for the overpopulation of ion B states induced by radiation absorption. At present we are not aware of such an additional channel.

Inspection of table 1 shows also that the ratio of rate constants by  $O_2$  and by  $N_2$  is also class-dependent. In the pulsed discharge method it amounts to 2.43, and decreases to 1.6 for electron beam methods down to 1.18 in the present work case. This might be

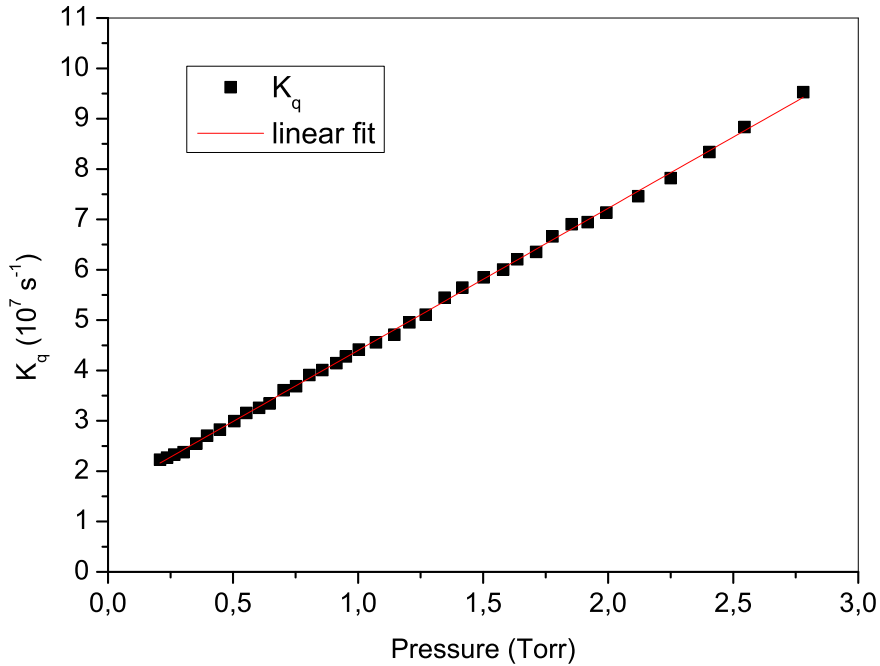


**Figure 7.** Stern-Volmer plot of the  $N_2^+(B^2\Sigma_u^+, v = 0)$  quenching rate in  $N_2 + 50\%O_2$ . The linear fit gives a slope of  $(2.8236 \pm 0.0128) \times 10^7 \text{ Torr}^{-1} \text{ s}^{-1}$  and an intercept of  $(1.5752 \pm 0.0178) \times 10^7 \text{ s}^{-1}$ . The inverse of the intercept,  $\tau = 63.48 \pm 0.72 \text{ ns}$  is in good agreement with the 62.33 ns radiative lifetime of [24].

the spy of the influence of changing conditions on the rate coefficient results in indirect, non-selective methods. In continuous charged particles beam or X-ray excitation, this may be the effect of a non exact calculation of secondary electrons excitation. In pulsed discharge methods, the discharge decay time can influence the measured quenching of the excited species, and the addition of oxygen may shorten the discharge decay, allowing the measurement of faster rate coefficients. An analogous difficulty of the pulsed discharge method in recovering fast decay times was perhaps already evidenced in the measurement of  $N_2(C^3\Pi_u, v)$  of [6] compared to the same measurements by LIF of our group [9]. The two data sets agree well for  $v=0, 1$  and  $2$ , showing increasing values of the rate coefficients up to about  $4.3 \times (10^{-11} \text{ cm}^3 \text{ s}^{-1})$ , but for  $v=3$  the value of [6] remains slightly lower than that of  $v=2$ , while the LIF measurement shows an increase to  $6.34 \times (10^{-11} \text{ cm}^3 \text{ s}^{-1})$  and confirm the increasing trend with a  $9.86 \times (10^{-11} \text{ cm}^3 \text{ s}^{-1})$  value for  $v=4$ .

#### 4. Conclusions

We have measured by laser induced fluorescence the rate coefficients of  $N_2^+(B^2\Sigma_u^+, v = 0)$  collision quenching by  $N_2$  and  $O_2$ . The present results agree well with literature data

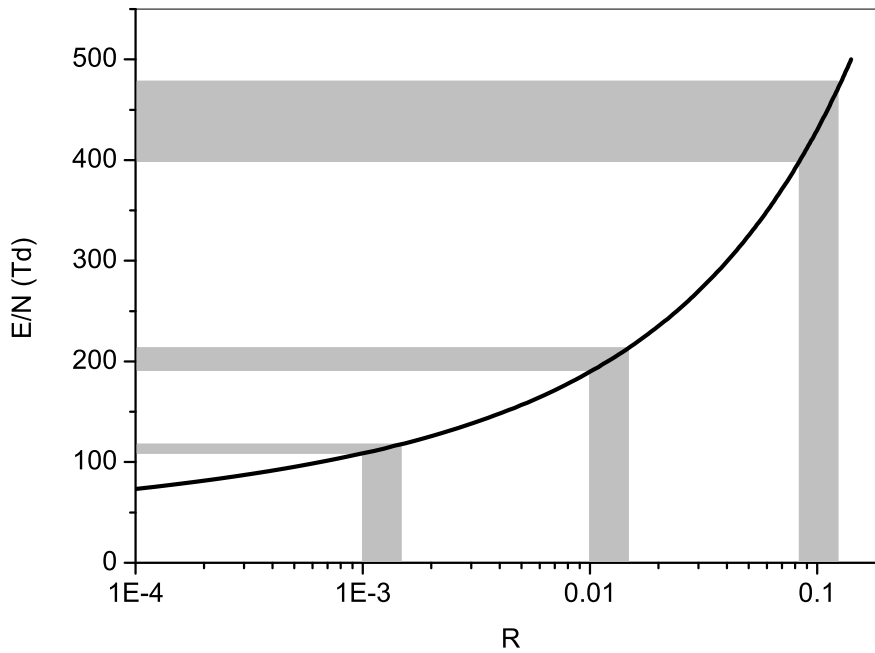


**Figure 8.**  $E/N$  vs.  $R = r_2/r_1$  calculated by BOLSIG+ in pure  $N_2$ . Three uncertainty cases are presented, with  $R$  ranging from  $10^{-3}$  to  $1.47 \times 10^{-3}$ , and from  $10^{-2}$  to  $1.47 \times 10^{-2}$  and from  $8.3 \times 10^{-2}$  to  $1.23 \times 10^{-1}$ . The cross sections are taken from [25] and from [26] for processes (1) and (2) respectively.

obtained by selective methods for ion B state excitation. These data are compared to collision data obtained by various further non-selective methods. Possible systematic conceptual errors relevant to three classes of measurement methods are briefly discussed. Selective methods appear to be at present conceptually more reliable, but, in the absence of a definitive confirmation, we must accept an indetermination in these values with a preference, we believe, for selective methods results. A precise knowledge of these collision quenching data is very important when spectroscopic methods that employ the ratio of FNS and SPS emissions are applied to the estimation of the reduced electric field in an electrical discharge at high pressure. The effect of such an indetermination has been briefly analyzed for a nitrogen discharge at atmospheric pressure.

## 5. References

- [1] Gallimberti I, Hepworth J K and Klewe R C 1974 *J. Phys. D: Appl. Phys.* **7** 880–898
- [2] Isola L M, Gomez B J and Guerra V 2010 *J. Phys. D: Appl. Phys.* **43** 015202
- [3] Hoder T, Sira M, Kozlov K V and Wagner H E 2008 *J. Phys. D: Appl. Phys.* **41** 035212
- [4] Hagelaar G J M and Pitchford L C 2005 *Plasma Sources Sci. Technol.* **14** 722 – 733
- [5] Paris P, Aints M, Valk F, Plank T, Haljaste A, Kozlov K V and Wagner H E 2005 *J. Phys. D: Appl. Phys.* **38** 3894–3899
- [6] Pancheshnyi S, Starikovskaia S and Starikovskii A 2000 *Chem. Phys.* **262** 349–357
- [7] Pancheshnyi S V, Starikovskaia S M and Starikovskii A Y 1998 *Chem. Phys. Lett.* **294** 523–527
- [8] Pancheshnyi S 2006 *J. Phys. D: Appl. Phys.* **39** 1708–1710
- [9] Dilecce G, Ambrico P F and De Benedictis S 2006 *Chem. Phys. Lett.* **431** 241 – 246

- [10] Dilecce G, Ambrico P F and De Benedictis S 2007 *Plasma Sources Sci. Technol.* **16** 511 – 522
- [11] Jolly J and Plain A 1983 *Chem. Phys. Lett.* **100** 425–428
- [12] Tellinghuisen J B, Winkler C A, Freeman C G, McEwan M G and Phillips L F 1970 *J. Chem. Soc. Faraday Trans. II* **68** 833–838
- [13] Comes F J and Speier F 1969 *Chem. Phys. Lett.* **4** 13
- [14] Brocklehurst B and Downing F A 1967 *J. Chem. Phys.* **46** 2976–2991
- [15] Hirsh M N, Poss E and Eisner P N 1970 *Phys. Rev. A* **1** 1615–1626
- [16] Mackay G I and March R E 1971 *Can. J. Chem.* **49** 1268–1271
- [17] Belikov A E, Kusnetsov O V and Sharafutdinov R G 1995 *J. Chem. Phys.* **102** 2792–2801
- [18] Chen C H, Payne M G, Hurst G S and Judish J P 1976 *J. Chem. Phys.* **65** 3863–3868
- [19] Mitchell K B 1970 *J. Chem. Phys.* **53** 1795–1802
- [20] Johnson A W and Fowler R G 1970 *J. Chem. Phys.* **53** 65–72
- [21] Dilecce G, Ambrico P and De Benedictis S 2007 *Plasma Sources Sci. Technol.* **16** S45–S51
- [22] Luque J and Crosley D 1999 Int. rep. p99-009 Tech. rep. SRI
- [23] Pintassilgo C D, Guaitella O and Rousseau A 2009 *Plasma Sources Sci. Technol.* **18** 025005
- [24] Gilmore F, Laher R R and Espy P J 1992 *J. Phys. Chem. Ref. Data* **21** 1005–1107
- [25] Simek M 2002 *J. Phys. D: Appl. Phys.* **35** 1967 – 1980
- [26] Borst W L and Zipf E C 1970 *Phys. Rev. A* **1** 834–840